

Multiple Electron Beams Generated by a Helicon Plasma Discharge

Robert Tseng Shiung Chen and Noah Hershkowitz

*Engineering Research Center for Plasma-Aided Manufacturing, University of Wisconsin-Madison,
Madison, Wisconsin 53706-1608*

(Received 6 February 1998)

Simultaneous electron beams with different energies were directly detected by Langmuir probes in a steady state helicon plasma discharge. The probe-detected electron-beam velocities were in good agreement with the phase velocities of the multimode helicon waves. [S0031-9007(98)06154-7]

PACS numbers: 52.50.Dg, 52.35.Hr, 52.70.-m

Helicon waves are of considerable interest because they can be used to achieve very high plasma densities with very high fractional ionization in low magnetic field, electrodeless discharges [1–3]. Both theoretical and experimental investigations have been conducted to understand the processes leading to high ionization [1–9]. It is generally believed that electron trapping by helicon waves generates energetic electrons which are effective at ionizing the plasma.

The existence of a trapping mechanism is supported by experimental evidence of fast electrons traveling at the phase velocity of the helicon wave. The first such evidence was provided by Zhu and Boswell [2], who constructed a pulsed argon ion laser based on a high density helicon discharge. The intensity variation of Ar^{++} and Ar^+ lines indicated a population of fast electrons in the 15–50 eV range, in agreement with the range of electron energy deduced from measured wavelengths. They also reported a transient bump-on-tail feature in the electron energy distribution function which disappeared 1 μs after initiation of the pulse and was not present at later times. Komori *et al.* [3] and Loewenhardt *et al.* [4] have also investigated the mechanism in pulsed helicon plasmas. Their data showed that the most rapid increase in electron density or electron temperature was correlated with the maximum damping rate estimated by linear Landau damping theory [5]. In the latter experiment, Langmuir probe data sampled from a toroidal pulsed plasma also suggested the existence of a bump-on-tail feature, consistent with the helicon phase velocity measurement. Chen and Decker [6] inferred the existence of fast electrons from the floating potential of an end plate inserted at the end of a helicon plasma away from the antenna. Recently, Ellingboe *et al.* [7] detected a strong radio frequency (rf) modulation of an Ar^+ line emission peak in a helicon plasma. At each cycle, the emission peak was found to propagate axially at a velocity equal to the phase velocity of the helicon wave, suggesting an energetic electron group moving with that velocity. More recently, Molvik *et al.* [8] detected a 20 eV electron beam with an electron energy analyzer in their helicon plasma source, and the electron beam velocity was found to be in agreement with the phase velocity of the helicon wave.

Theoretical analysis of helicon plasmas with nonuniform radial density profiles suggests that a variety of radial and azimuthal wave modes can be excited [10]. In addition, previous experiments [11] have found beat modes (previously identified as standing waves) in helicon plasmas indicating the simultaneous presence of several azimuthal and radial modes corresponding to the fundamental rf and to the second harmonic as well. Wave electron trapping is expected for each of the simultaneous modes. Since each mode corresponds to a different phase velocity, several electron beams with different velocities are expected.

In this Letter, we present Langmuir probe data showing the simultaneous presence of several electron beams with different energies in a steady state helicon plasma source. The electron beam energies are found to agree with the phase velocities of the experimentally measured multimode helicon waves. We believe this is the first report of such phenomena in a helicon plasma source.

The steady state helicon plasma source, described in detail elsewhere [11], used a Nagoya type III antenna [12] to excite helicon waves in a 10 cm i.d., 152 cm long Pyrex tube immersed in a uniform axial dc magnetic field. The right end of the tube is connected to a larger vacuum chamber. Continuous rf wave power transmitted to the antenna at 13.56 MHz could be varied up to 1.3 kW. Argon plasmas were studied with electron temperature $T_e = 3\text{--}5$ eV, density $n_e = 10^{12}\text{--}10^{13}$ cm^{-3} , neutral pressure 4–35 mTorr, and axial dc magnetic field $B_0 = 400\text{--}500$ G. A deep blue core (from ion emission) indicated the presence of strong ion excitation in the discharge associated with helicon waves.

A cylindrical Langmuir probe with an rf-shielded probe shaft and a B -dot probe were used to detect the fast electrons and the helicon waves, respectively. The axis of the Langmuir probe was oriented perpendicular to the axial dc magnetic field B_0 . All of the probe data were taken in an axial (z) position range of $z = 17$ to 47 cm ($z = 0$ was at the antenna midplane). The probe provided time averaged currents in the presence of rf. No rf filters at 13.56 MHz and its harmonics were used. The collecting probe tips were cylindrical graphite rods with radius $a = 0.15\text{--}0.3$ mm and 1.5–2 mm in length. Since electron Debye lengths were typically less than 0.01 mm,

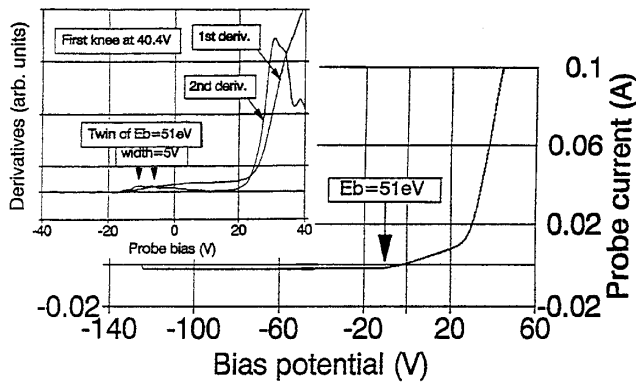


FIG. 1. A typical Langmuir probe I - V trace which shows the presence of energetic electrons in addition to a Maxwellian bulk plasma. The rf perturbation measured in this case was about 5 V.

i.e., $\lambda_D \ll a$, the probe could be treated as a planar probe. The B -dot probe was used to measure the axial component of the amplitude of B_z of the helicon wave fields just outside the discharge tube. The B -dot probe used a surface signal pickup coil, with axis oriented parallel to the z direction. The coil was introduced perpendicular to the Pyrex cylinder (at $r \approx 6$ cm) through perforations in an aluminum shield which shielded the rf from the laboratory. The B -dot probe data were taken in the range of $z = 15$ to 57 cm. The experimental uncertainty in the amplitude of the fluctuating B_z field was the order of $\pm 5\%$.

A representative Langmuir probe current-voltage (I - V) characteristic is shown in Fig. 1. These data show the presence of energetic electrons (with energies up to 51 eV) in addition to a background (Maxwellian) plasma with electron temperature $T_e = 3$ eV. The energetic electrons contribute a straight-line portion to the I - V curve.

Planar probe theory shows that, in a plasma without rf perturbations (i.e., a dc plasma), the presence of monoenergetic electrons results in a straight-line region [13]. If the electrons are all directed in one direction (i.e., along the dc B_0 field), the beam contributes a constant additional current for bias voltages more positive from $-E_b/e$, where E_b is the beam energy. If the high energy electrons are isotropic, they contribute a sloping straight-line portion for bias voltages more positive than $-E_b/e$. If the energetic electrons are anisotropic but have a range in energy, an approximate straight-line I - V characteristic might still result. When two different fast electron groups are present, they result in two straight-line regions with different slopes to the left of V_p , etc. The easiest way to identify the presence of the energetic electrons is to look at the second derivative of the I - V curve. In all cases, the second derivative has a peak at the maximum beam energy.

In the presence of rf, the time averaged I - V characteristics of Maxwellian plasmas with electron beams can be changed substantially [14,15]. For a Maxwellian plasma,

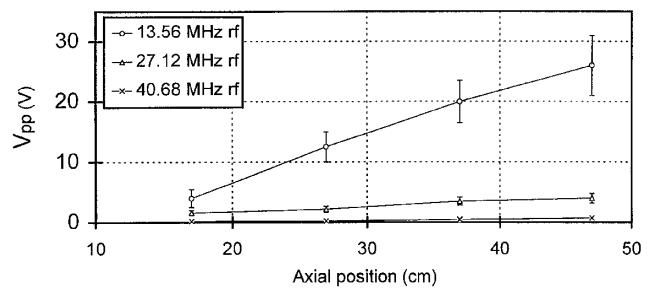


FIG. 2. Capacitive probe measurements of the averaged peak-to-peak voltage (V_{pp}) of rf perturbation on axis of, and along, the plasma column for the first three rf harmonics at a typical discharge condition: Neutral Ar pressure $P_n = 19.38$ mTorr, dc magnetic field $B_0 = 400$ G, and rf power $P_{rf} = 1.1$ kW.

a two knee zone with potential width equal to the peak-to-peak rf plasma amplitude (V_{pp}) is induced around the dc V_p by the rf perturbation. Similarly, the rf perturbation also results in a curved-line transition region with potential width V_{pp} between straight-line portions associated with beams. In this case, the second derivative in the transition region has two twin peaks separated by V_{pp} . It follows that the beam energy is given by the potential difference between the left bump of the twin (i.e., the one with more negative bias voltage) and the left knee. This valuable property is independent of the beam energy and current as well as the rf perturbation amplitude and frequency.

In order to obtain correct electron energy information from the second derivative curve, one must know the voltage amplitude of the rf perturbation. Figure 2 gives V_{pp} taken by a capacitive probe, located at approximately the discharge tube axis, for the fundamental and the first two harmonics measured along the steady state discharge.

Nonsinusoidal spatial helicon beat waveforms with very good repeatability were detected by the B -dot probe measuring the B_z component along the axial direction at discharge conditions captioned in Fig. 3. Fast Fourier

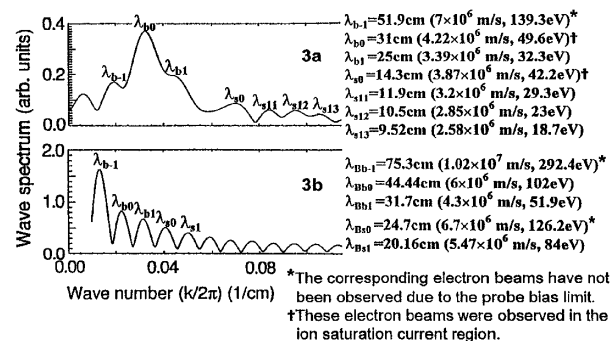


FIG. 3. The FFT wave power spectrum of the nonsinusoidal spatial helicon beat wave detected by a B -dot probe along the plasma column at discharge conditions of (a) $P_n = 19.38$ mTorr, $B_0 = 400$ G, and $P_{rf} = 1.1$ kW (where $\lambda_{s,11}$ and $\lambda_{s,13}$ are split components of $\lambda_{s,12}$ [10]), and (b) $P_n = 25$ mTorr, $B_0 = 450$ G, and $P_{rf} = 600$ W.

transform (FFT) was used to determine the wave spectrum of the spatial beat waveforms. The helicon mode and frequency of every wave packet were identified numerically by comparison to the dispersion relation derived for helicon waves in a radially nonuniform plasma [10]. The helicon phase velocity can thus be calculated from the wavelength and the identified frequency following the method given in Ref. [11]. The FFT spectrum of the beat waveforms in our experiments are shown in Fig. 3. The center wavelength of a wave packet which was at the fundamental frequency (13.56 MHz) and belongs to the $m = 0, p = 1$ mode is designated λ_{b0} , and λ_{s1} designated the center wavelength of a wave packet which was at 27.12 MHz and belong to the $m = 1, p = 0$ mode, etc. The wavelength, the wave phase velocity, and the electron energy (deduced from the phase velocity) are given on the right side of the figures.

The Langmuir probe measurements were taken at $r = 0$ with the same plasma conditions as the B-dot probe measurements. Figures 4(a), 4(c), and 4(e) show the time averaged Langmuir probe I - V characteristics taken at three different axial locations of the plasma column under the same discharge conditions of Fig. 3(a), where 4(a) shows clearly defined sloping straight lines, indicating the presence of two fast electron groups. The associated second derivative curves are shown in Figs. 4(b), 4(d), and 4(f), respectively.

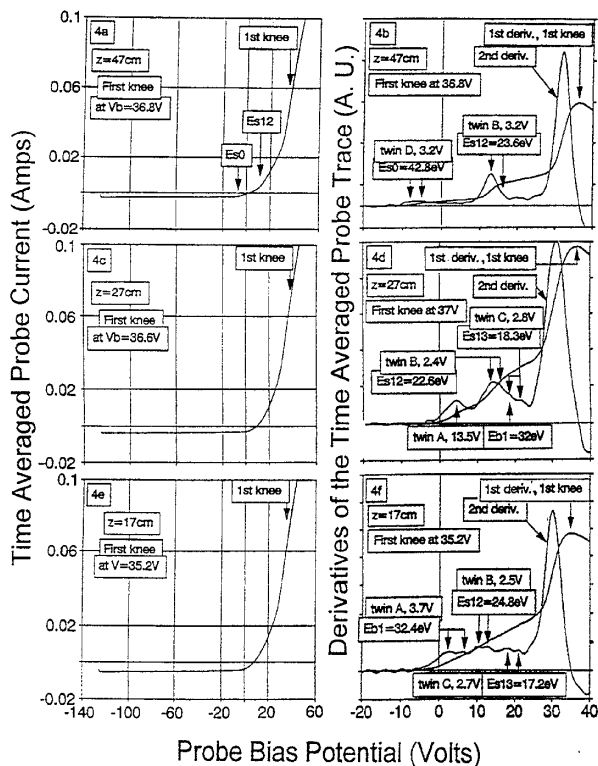


FIG. 4. (a) to (f): The time averaged probe I - V characteristics (left side) and their first and second derivatives (right side) taken on axis at three axial (z) positions along the plasma column under the same discharge conditions captioned for Fig. 3(a).

We use the derivative curves to identify the electron beams for probe data shown in Figs. 4(c) and 4(e). Consider the data in Fig. 4(e), taken at $z = 17$ cm. Three twin peaks appear on the tail (indicated by the pairs of arrows) of the second derivative curve shown in Fig. 4(f), indicating three electron beams. Comparing the twin widths (3.7 V for twin A; 2.5 V for twin B; 2.7 V for twin C) with the measured rf perturbation V_{pp} at $z = 17$ cm (4 V for 13.56 MHz; 1.7 V for 27.12 MHz, Fig. 2), we established that twin A was generated by a helicon wave at 13.56 MHz, twin B and twin C were generated by waves at 27.12 MHz. By measuring the potential difference between the first bump of the twin and the first knee, the beam energies were determined as $E_{b1} = 32.4$ eV (twin A), $E_{s12} = 24.8$ eV (twin B), and $E_{s13} = 17.2$ eV (twin C). Comparing these energies with the helicon wave phase velocity measurements [Fig. 3(a)], we found that E_{b1} was consistent with the dominant wave mode at λ_{b1} which generates an electron beam of 32.3 eV; E_{s12} was consistent with the mode at λ_{s12} which generates an electron beam of 23 eV; E_{s13} was consistent with the mode at λ_{s13} which generates an electron beam of 18.7 eV.

Data shown in Fig. 4(c) were taken at $z = 27$ cm. The same beams (twins A, B, C) were observed on its second derivative curve shown in Fig. 4(d). Note that the width of twin A ($= 13.5$ V) becomes wider than the other two since V_{pp} ($= 12.5$ V) of 13.56 MHz at $z = 27$ cm become stronger (Fig. 2). Twin B became asymmetric (due to the effect of nonsinusoidal rf). Twin C became weak. The right bump of twin A overlapped with the left bump of twin C, making the resulted bump higher than both twin A and twin C. The beam energies were in very good agreement with energies deduced from helicon phase velocities [Fig. 3(a)].

Data shown in Fig. 4(a) were taken at $z = 47$ cm. In its second derivative [Fig. 4(b)], twin B could still be

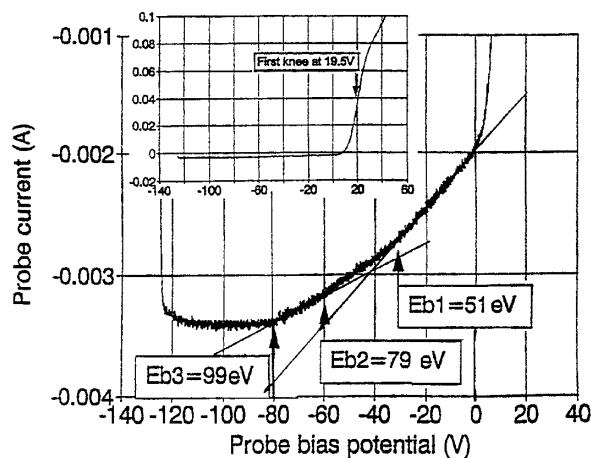


FIG. 5. The magnified time averaged Langmuir probe I - V curve in the ion saturation current region which was taken at the same discharge conditions captioned for Fig. 3(b). The whole I - V probe trace is shown by the inset.

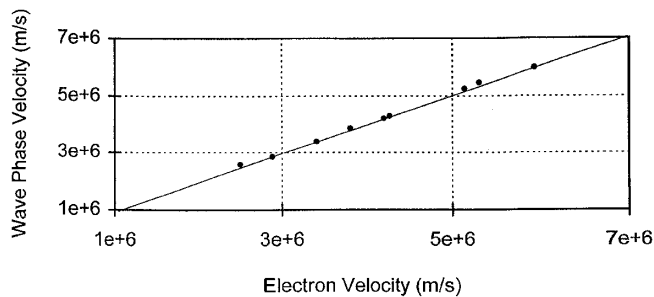


FIG. 6. The electron-beam velocities detected by a Langmuir probe versus the central (or average) helicon wave phase velocities detected by the B -dot probe.

observed but appeared more asymmetric. Note that twin A could not be observed anymore. The beam driven by the dominant $b1$ mode is dissipated before $z = 47$ cm. This could also be seen from the blue core, indicating the strong excitation in the discharge, which started from $z = 10$ cm and ended at about $z = 42$ cm. The beam driven by the dominant $b1$ mode strongly interacts with the background plasma, since electrons with $E_{b1} = 32.3$ eV have much larger ionization cross sections with the neutral argon atoms resulting in greater excitation of ion states than those with $E_{s12} = 22.4$ eV [16]. The I - V curves showed that the E_{b1} beam was approximately 1.6 times greater in amplitude than the E_{s12} beam in the region of $z < 22$ cm. Twin D has a width of 3.2 V, so it was driven by a wave of 27.12 MHz (with $V_{pp} = 3.9$ V, Fig. 2). The beam energy $E_{s0} = 42.8$ eV was consistent with the electron energy 42.2 eV ($s0$ mode) deduced from the helicon phase velocity.

The probe data shown in Fig. 5 were taken at the discharge conditions of Fig. 3(b). Figure 5 is a typical type averaged I - V curve which was highly magnified and shows clearly defined beam information in the ion saturation current region. The good identifiability is due to the fact that the beam energies were not only much greater than the rf perturbation energy eV_{pp} (~ 8 eV in this case) but also very far from the strong bulk plasma information. The beam information could be directly determined graphically from the time averaged I - V curve without using its derivatives. The beam energies $E_{b1} =$

51.3 eV, $E_{s1} = 79.3$ eV, and $E_{b0} = 99.3$ eV agreed with energies (51.9, 84, 102 eV) deduced from helicon wave modes (λ_{b1} , λ_{s1} , and λ_{b0}), respectively [Fig. 3(b)].

Figure 6 summarizes the comparison between the Langmuir probe-detected beam velocities and the B dot probe-detected helicon phase velocities. The good agreement between these two velocities demonstrates that the simultaneous existence of multiple electron beams is caused by the simultaneous helicon wave modes.

The authors thank F.F. Chen for helpful discussions, and thank S. Gross and P.W. Sandstrom for their technical assistance. This work was supported by NSF Grants No. EEC-8721545 and No. ECS-9529565.

- [1] R. W. Boswell, Phys. Lett. A **33**, 457 (1970); R. W. Boswell, Ph.D. thesis, Flinders University of South Australia, 1970.
- [2] Peiyuan Zhu and R. W. Boswell, Phys. Rev. Lett. **63**, 2805 (1989).
- [3] A. Komori *et al.*, Phys. Fluids B **3**, 893 (1991).
- [4] P. K. Loewenhardt *et al.*, Phys. Rev. Lett. **67**, 2792 (1991).
- [5] F. F. Chen, Plasma Phys. Controlled Fusion **33**, 339 (1991).
- [6] F. F. Chen and C. D. Decker, Plasma Phys. Controlled Fusion **34**, 635 (1992).
- [7] A. R. Ellingboe *et al.*, Phys. Plasmas **2**, 1807 (1995).
- [8] A. W. Molvik, A. R. Ellingboe, and T. D. Rognlien, Phys. Rev. Lett. **79**, 233 (1997).
- [9] B. M. Harvey and C. N. Lashmore-Davies, Phys. Fluids B **5**, 3864 (1993).
- [10] F. F. Chen, M. J. Hsieh, and M. Light, Plasma Sources Sci. Technol. **3**, 49 (1994).
- [11] R. T. S. Chen *et al.*, Plasma Sources Sci. Technol. **4**, 337 (1995).
- [12] S. Okamura *et al.*, Nucl. Fusion **26**, 1491 (1986).
- [13] N. Hershkowitz, in *Discharge Parameters and Chemistry*, edited by O. Auciello and D. L. Flamm, Plasma Diagnostics Vol. I (Academic, New York, 1989), p. 113.
- [14] N. Hershkowitz *et al.*, Plasma Chem. Plasma Process. **8**, 35 (1988).
- [15] K. N. Leung, T. K. Samec, and A. J. Lamm, Phys. Lett. A **51**, 490 (1975).
- [16] For instance, D. Rapp and P. Englander-Golden, J. Chem. Phys. **43**, 1464 (1965).